PID Controller Design for MIMO Systems
by Applying Balanced Truncation to Integral-Type Optimal Servomechanism

Yoshimasa Ochi* and Nobuhiro Yokoyama*

*National Defense Academy, Yokosuka, 239-8686
Japan (e-mail: ochi@nda.ac.jp, yoko@nda.ac.jp).

Abstract: A closed-loop balanced truncation technique has been applied to an integral-type optimal servomechanism (IOS) expressed in graph-operator form of normalized right coprime factorization to produce a reduced-size state-feedback gain matrix, which is then converted into proportional-derivative (PD) gain matrices. On the other hand, the states of the integral of control error in the IOS are not truncated, so that the feedback gain matrix of the IOS for the states becomes the integral (I) gain matrix. All the design procedure is completed with the state-space approach, which is convenient especially in dealing with multiple-input multiple-output (MIMO) systems. Application of the proposed method to the boiler system of the PID '12 benchmark problem demonstrates the effectiveness of the design method.

Keywords: PID control, MIMO systems, Controller reduction, Balanced truncation, Normalized right coprime factorization, Integral-type optimal servomechanism, Boilers

1. INTRODUCTION

Model-based proportional-integral-derivative (PID) control synthesis is a typical low-order controller design problem. As well known, there are three approaches to design of a low-order controller: 1) first reduce a given plant, and then design a controller using the reduced plant, 2) first design a high-order controller using a given plant, and then reduce the controller to a lower-order controller, 3) directly find a low-order controller using the original plant. Conventionally, the second approach has often been taken, since it is considered that the model error due to plant reduction results in degrading performance of the low-order controller (Anderson and Liu, 1989). Although this is true in general, it depends on the reduction method employed. In fact, the first approach is useful, when the plant is appropriately reduced. Particularly for the controller design purpose, closed-loop model reduction provides a more desirable plant model than open-loop model reduction (Codrons, 2005).

The present author proposed a simple and effective design method of a single-input single-output (SISO) PID controller using the first approach, where the ν-gap (Vinnicombe, 1993) is taken as a criterion representing the plant-model reduction error in the closed-loop sense (Ochi and Kondo, 2010). A problem with the method is that it is difficult to extend to MIMO systems because of the increase of the number of plant parameters. In practice of PID control, MIMO systems are usually modelled as a set of SISO systems and a decentralized control system is constructed with the controllers designed for each SISO system, where cross-coupling among plant variables are ignored and design procedure tends to be complicated, often accompanying decoupling control or numerical optimization (Åström and Hägglund, 2006; Johnson and Moradi, 2005; Silva and Erraz,

2006). On the other hand, centralized controller synthesis was considered using the state-space design approaches such as pole placement, linear quadratic regulator (LQR), or H_∞ control (Seraji, 1980; Zheng, Wang, and Lee, 2002). However, those methods are not necessarily simple or efficient, accompanying calculation with the Laplace operator or using an iterative algorithm. In contrast, the design method recently proposed by the present author is simple and efficient (Kondo, Ochi, and Sasano, 2011). The method employs fractional balanced reduction (FBR) (Mayer, 1990), a closed-loop model reduction method, for plant reduction, followed by state transformation and design of an integral-type optimal servomechanism (IOS) (Smith and Davison, 1972). Note that both FBR and IOS are state-space based methods, which significantly facilitates MIMO control synthesis. Although Suh and Yang (2005) also applied IOS to PID controller design, the plant considered was a SISO second-order system.

The present paper proposes another design method base on IOS and FBR, in which an IOS designed for a given plant is reduced, instead of the plant. More specifically, balanced truncation (BT) (Moore, 1981) has been applied to the IOS to produce a reduced-size state-feedback gain matrix, which is then converted into proportional-derivative (PD) gain matrices, whereas the states for the integral of control error in the IOS are not truncated, so that the corresponding feedback gain matrix of the IOS itself becomes the integral (I) gain matrix. The design method also requires neither iterative algorithm nor numerical optimization. The difference from the method by plant reduction is that FBR is used for controller (feedback gain matrix) reduction, although a reduced-order plant is also obtained simultaneously and used in the design. Numerical simulation and stability analysis have been conducted using the plant model of the benchmark problem (Benchmark PID 2012) (Morilla, 2011a, b).

2. CONTROLLER DESIGN

2.1 Integral-Type Optimal Servomechanism

Consider a linear plant model given by

$$\dot{x} = Ax + Bu,\qquad(1)$$

$$y = [y_I^T\ y_P^T\ y_{PD}^T]^T = [C_I^T\ C_P^T\ C_{PD}^T]^T x = Cx \qquad(2)$$

where $x\in\Re^n$, $u\in\Re^m$, and $y\in\Re^p$ are the state vector, the input vector, and the output vector, respectively. The outputs to which P, I, or D action is applied are defined in Table 1. $y_P\in\Re^{p_P}$ and $y_D\in\Re^{p_D}$ are the outputs for P action only and PD action, respectively. P action is applied to all the outputs.

Table 1 Definition of the output vectors

Action	P	I	D
Outputs	$y\in\Re^P$	$y_I\in\Re^{p_I}$	$y_D\in\Re^{p_D}$
$y_I\in\Re^{p_I}$	✓	✓	
	✓	✓	✓
$y_P\in\Re^{p_P}$	✓		
$y_{PD}\in\Re^{p-p_I-p_P}$	✓		✓

The matrices, A, B, and C are constant matrices of appropriate size, and it is assumed that this system is controllable, C is of row full rank, and (A, C) is observable.

Define the control error, $e = r - y_I$, and its integral,

$$\varepsilon = \int e\,d\tau,\qquad(3)$$

where $r\in\Re^{p_I}$ is a constant reference-output vector. Then, define the following augmented system:

$$\dot{x}_a = A_a x_a + B_a u + B_r r,\qquad(4)$$

where $x_a = [x^T\ \varepsilon^T]^T$,

$$A_a = \begin{bmatrix} A & 0 \\ -C_I & 0 \end{bmatrix},\ B_a = \begin{bmatrix} B \\ 0 \end{bmatrix},\ B_r = \begin{bmatrix} 0 \\ I_{p_I} \end{bmatrix},$$

and I_p is a $p\times p$ identity matrix. Also, define the cost function:

$$J = \int_0^\infty (x^T Q_x x + \varepsilon^T Q_\varepsilon \varepsilon + u^T R u)dt,\qquad(5)$$

where $Q_x = C^T Q_y C$ and $R = I_m$. Further, The weighting matrices given as $Q_y = \mathrm{diag}(q_{y1}^2, \ldots, q_{yp}^2)$, $Q_\varepsilon = \mathrm{diag}(q_{\varepsilon 1}, \ldots, q_{\varepsilon p_I})$ are positive-definite, where $\mathrm{diag}(\cdot)$ denotes a diagonal matrix. The LQR theory gives the optimal control law that minimizes the cost function, i.e.,

$$u = K_a x_a,\qquad(6)$$

where $K_a = [K_x\ K_\varepsilon]$ is given by

$$K_a = -B_a^T X_a.\qquad(7)$$

In (7), X_a is the positive-definite solution of the algebraic Riccati equation:

$$X_a A_a + A_a^T X_a - X_a B_a B_a^T X_a + Q_a = 0,\qquad(8)$$

where Q_a is a block-diagonal matrix comprsing Q_x and Q_ε. The closed-loop system is then expressed as

$$\dot{x}_a = A_{acl} x_a + B_r r,\qquad(9)$$

where

$$A_{acl} = A_a + B_a K_a = \begin{bmatrix} A+BK_x & BK_\varepsilon \\ -C_I & 0 \end{bmatrix}.\qquad(10)$$

The output equation can be written as

$$y = [C\ 0]\,[x^T\ \varepsilon^T]^T.\qquad(11)$$

2.2 Reduction of IOS by BT

The IOS designed above is reduced to an integral-preceded-by-proportional-derivative (I-PD) controller by applying BT to a subsystem of the IOS as follows.
First, define the weighted output vector:

$$y_{aw} := \begin{bmatrix} y_w \\ \varepsilon_w \end{bmatrix} := \begin{bmatrix} C_w & 0 \\ 0 & Q_\varepsilon^{1/2} \end{bmatrix}\begin{bmatrix} x \\ \varepsilon \end{bmatrix} =: C_{aw} x_a,\qquad(12)$$

where $C_w = Q_y^{1/2}C$. Then, consider the system described by (4) and (12), and represent in the normalized right coprime factorization (NRCF) form as

$$y_{aw}(s) = N(s)M(s)^{-1}u(s),\qquad(13)$$

where $N(s)$ and $M(s)$ are given by

$$\begin{bmatrix} N(s) \\ M(s) \end{bmatrix} = \begin{bmatrix} C_{aw} \\ K \end{bmatrix}(sI_{n+p} - A_{acl})^{-1}B_a + \begin{bmatrix} 0 \\ I_m \end{bmatrix} =: \begin{bmatrix} A_{acl} & B_a \\ \hline C_{aw} & 0 \\ K & I_m \end{bmatrix}.\qquad(14)$$

Balancing the system requires positive-definite solutions of the following Lyapunov equations:

$$XA_{acl} + A_{acl}^T X + [C_{aw}^T\ K^T][C_{aw}^T\ K^T]^T = 0,\qquad(15)$$

$$YA_{acl}^T + A_{acl}Y + B_a B_a^T = 0.\qquad(16)$$

Equation (15) is a Lyapunov equation with respect to X, which is observability Gramian, and (16) is a Lyapunov equation with respect to Y, which is controllability Gramian. The solutions, X and Y, are positive definite matrices, because A_{acl} is a stable matrix. Note that (15) is equivalent to (8), which is proved by substituting (7) into (8) and using the definition of Q_a. Hence, $X_a = X$ and $K_a = K$ hold.

In FBR, the balanced system is truncated by removing the subsystem for the state variables corresponding to smaller Hankel singular values. In the I-PD controller design, however, only the subsystem of (14) corresponding to the state vector x is balanced and truncated as follows (Schelfhout and Moor, 1996), since the state vector ε should appear for integral action in the resulting control law.

Let the state transformation matrix for balancing the subsystem be T_x and define the entire transformation matrix:

$$T = \begin{bmatrix} T_x & 0 \\ 0 & I_{p_I} \end{bmatrix},\qquad(17)$$

Let the balanced state vector for the subsystem be x_{bl}, which is defined as $x_{bl} = T_x^{-1}x$. The following procedure gives T_x.

1) Solve (15) and (16) for X and Y, respectively, and partition the solutions as

$$X = \begin{bmatrix} X_x & X_{x\varepsilon} \\ X_{x\varepsilon}^T & X_\varepsilon \end{bmatrix} \text{ and } Y = \begin{bmatrix} Y_x & Y_{x\varepsilon} \\ Y_{x\varepsilon}^T & Y_\varepsilon \end{bmatrix},$$

   where X_x and Y_x are $n\times n$ positive-definite matrices and X_ε and Y_ε are $p_I\times p_I$ positive-definite matrices.

2) Diagonalize X_x and Y_x, i.e., find the orthogonal matrices, V_X and V_Y, and the diagonal matrices, Λ_X and Λ_Y, satisfying $X_x = V_X\Lambda_X V_X^T$ and $Y_x = V_Y\Lambda_Y V_Y^T$.

3) Define $H_x = \Lambda_Y^{1/2}V_Y^T V_X\Lambda_X^{1/2}$.

4) Decompose H_x into its singular value decomposition as $H_x = U_x\Sigma_x W_x^T$, where U_x and W_x are $n\times n$ orthogonal matrices and $\Sigma_x = \mathrm{diag}(\sigma_i)$, where $\sigma_i > \sigma_j$ for $i < j$.

5) Compute $T_x = V_X\Lambda_X^{-1/2}U_x\Sigma_x^{1/2}$.

Substituting T_x into (17) and transforming the state variables yields the following balanced system:

$$\left[\begin{array}{c} N(s) \\ \hdashline M(s) \end{array}\right] = \left[\begin{array}{c|c} T^{-1}A_{acl}T & T^{-1}B_a \\ \hline C_{aw}T & 0 \\ \hline K_aT & I_m \end{array}\right] = \left[\begin{array}{c|c:c} T_x^{-1}A_{xcl}T_x & T_x^{-1}BK_\varepsilon & T_x^{-1}B \\ \hdashline -CT_x & 0 & 0 \\ \hline C_wT_x & 0 & 0 \\ 0 & Q_\varepsilon^{1/2} & 0 \\ \hline K_xT_x & K_\varepsilon & I_m \end{array}\right]$$
(18)

where $A_{xcl} = A + BK_x$. Partition the transformed state vector as $x_{bl} = T_x^{-1}x =: [x_{blL}^T \ x_{blS}^T]^T$, and let the dimension of x_{blL} be n_r ($< n$). Removing the subsystem regarding the state vector, x_{blS}, from the system, (18), gives the reduced system:

$$\left[\begin{array}{c} N_r(s) \\ \hdashline M_r(s) \end{array}\right] := \left[\begin{array}{c|c:c} A_{xclr} & B_{xr}K_\varepsilon & B_{xr} \\ \hdashline -C_{xr} & 0 & 0 \\ \hline C_{wr} & 0 & 0 \\ 0 & Q_\varepsilon^{1/2} & 0 \\ \hline K_{xr} & K_\varepsilon & I_m \end{array}\right]$$
(19)

Thus, the feedback gain matrix with the reduced size, $m \times (n_r + p_I)$, is obtained, i.e.,

$$K_r = [K_{xr} \ K_\varepsilon].$$
(20)

A reduced plant model of the original plant is also given by (A_{xr}, B_{xr}, C_{xr}), where $A_{xr} = A_{xclr} - B_{xr}K_{xr}$.

Remark: A notable feature of the above BT is that the output of the system to be reduced is chosen not to be y but to be y_{aw}, which makes the Lyapunov equation, (15), identical to the Riccati equation, (8). This feature is the same as that of FBR. In FBR, the augmented plant given by (4) and (12), where the external input r is disregarded, is represented as (14) in the form of NRCF. This NRCF representation called graph-operator form (Meyer, 1990) utilizes the LQR gain, K_a, given by (7) that minimizes the cost function, (5), or

$$J = \int_0^\infty (y_{aw}^T y_{aw} + u^T u)dt.$$
(21)

The cost function implies that the system described by (14) produces the amount of the output similar to that of the input in the sense of H_2 norm. This property is desirable for determining which state variables are influential not only on the outputs but also on the inputs given by the LQR or IOS control law. Hence, applying BT to the system given by (14) probably yields a good feedback gain matrix with a reduced size that approximately preserves the closed-loop properties of the original IOS. The performance degradation, which corresponds to the variation of the IOS due to the reduction, can be measured as the model error in BT, whose norm bounds are clearly given (Meyer, 1990; Vinnicombe, 1993).

2.3 Conversion into I-PD Control Law

Set the order of the reduced model to $n_r = p + p_D$, in order to define the state vector composed of the outputs and their derivative, i.e.,

$$z = \left[y^T \quad \dot{y}_D^T \right]^T.$$
(22)

where $y_D = C_{xrD}x_{blL}$, and C_{xrD} is a matrix comprising the rows of C_{xr} corresponding to y_D. Equation (22) can be rewritten as

$$z = M_s x_{blL} + N_s u,$$
(23)

where

$$M_s = \left[C_{xr}^T \quad (C_{xrD}A_{xr})^T \right]^T,$$
(24)

$$N_s = \left[0^T \quad (C_{xrD}B_{xr})^T \right]^T.$$
(25)

Under the assumption that M_s is non-singular, from (23), the state vector, x_{blL}, is given by

$$x_{blL} = M_s^{-1}(z - N_s u).$$
(26)

Define $u_{xr} := K_{xr}x_{blL}$ and $u_\varepsilon := K_\varepsilon \varepsilon$, and the IOS control law can approximately be written with the reduced state vector as

$$u = u_{xr} + u_\varepsilon.$$
(27)

From the definition of u_{xr} and (26), the following equation holds:

$$u_{xr} = K_{xr}M_s^{-1}\{z - N_s(u_{xr} + u_\varepsilon)\}.$$
(28)

Solving (28) for u_{xr} and substituting the solution into (27) yields the I-PD control law:

$$u = K_z z + K_{\varepsilon r}\varepsilon = K_P y + K_D \dot{y}_D + K_I \varepsilon,$$
(29)

where

$$K_z = EK_{xr}M_s^{-1} =: [K_P \ K_D],$$
(30)

$$K_{\varepsilon r} = EK_\varepsilon =: K_I,$$
(31)

$$E := (I_m + K_{xr}M_s^{-1}N_s)^{-1}.$$
(32)

The design procedure is summarized as follows:
1) Design an IOS using a given plant model, i.e., compute K_a in (7).
2) Solve the Lyapunov equations, (15) and (16).
3) Compute the transformation matrix, T_x, to obtain T.
4) Apply the state transformation to (14) to obtain (18).
5) Truncate the subsystem corresponding to the state vector, x_{blS}, to obtain the n_r ($= p + p_D$)-th-order system of (19).
6) Extract the state feedback gain matrix, K_r in (20), and the coefficient matrices of the reduced plant, A_{xr}, B_{xr}, and C_{xr} from (19).
7) Compute the PID gain matrices given by (30) and (31).

The I-PD control law can further be converted into proportional-integral-preceded-by-derivative (PI-D) and PID control laws ($y = y_D$), respectively, as

$$u = -K_P e + K_D \dot{y}_D + K_I \varepsilon,$$
(33)

$$u = -K_P e - K_D \dot{e} + K_I \varepsilon,$$
(34)

Note that this conversion does not affect the internal stability of the closed-loop system.

2.4 Design of I-P/PD Control Law

Set the order of the reduced model to $n_r = p$, and C_{xr} becomes a square matrix. Under the assumption that C_{xr} is non-singular, the state vector of the reduced plant is given by

$$x_{blL} = C_{xr}^{-1}y.$$
(35)

The integral-preceded-by-proportional (I-P) control law is then given by

$$u = K_P y + K_I \varepsilon,$$
(36)

where $K_P = K_{xr}C_{xr}^{-1}$ and $K_I = K_\varepsilon$. The I-P control law can also be converted into the PI control law:

$$u = -K_P e + K_I \varepsilon.$$
(37)

Designing an optimal servomechanism for (1) and (2), and following the design procedure provides the PD control law:

$$u = K_P e + K_D \dot{y}_D \quad \text{or} \quad u = -K_P e - K_D \dot{e}_D$$
(38)

Some remarks on the design method here may be in order:

1) The resulting controller preserves, if not perfectly, properties of the LQR, since IOS is a type of the LQR; namely, the controller provides the closed-loop system with adequate stability margins and good time responses.
2) Stability margins and control performance are easily traded off through selection of the weighting matrices of the quadratic cost function of the LQR.
3) As (29) suggests, the outputs used for P, I, and D actions do not need to be the same, although P action is applied to all the outputs. Therefore, if the outputs that can be measured but are not required to track reference outputs are available, those outputs should be used for P or PD-action, which makes the control system approximate to the 'state-feedback' one and consequently will improve stability.

3. APPLICATION TO PID'12 BENCHMARK PROBLEM

3.1 Linear Plant Model

The nonlinear state-space model of the boiler system considered in the benchmark problem is based on the following model given by Pellegrinetti and Bentsman (1996):

$$\dot{x}_1(t) = c_{11}x_4(t)x_1^{9/8}(t) + c_{12}u_1(t-\tau_1) - c_{13}u_3(t-\tau_3) + c_{14}, \quad (39)$$

$$\dot{x}_2(t) = c_{21}x_2(t) + [c_{22}u_2(t-\tau_2) - c_{23}u_1(t-\tau_1) \\ - c_{24}u_1(t-\tau_1)x_2(t)]/[c_{25}u_2(t-\tau_2) - c_{26}u_1(t-\tau_1)], \quad (40)$$

$$\dot{x}_3(t) = -c_{31}x_1(t) - c_{32}x_4(t)x_1(t) + c_{33}u_3(t-\tau_3), \quad (41)$$

$$\dot{x}_4(t) = -c_{41}x_4(t) + c_{42}u_1(t-\tau_1) + c_{43} + w_d(t), \quad (42)$$

$$y_1(t) = c_{51}x_1(t-\tau_4), \quad (43)$$

$$y_2(t) = c_{61}x_2(t-\tau_5), \quad (44)$$

$$y_3(t) = c_{70}x_1(t-\tau_6) + c_{71}x_3(t-\tau_6) \\ + c_{72}x_4(t-\tau_6)x_1(t-\tau_6) + c_{73}u_3(t-\tau_3-\tau_6) \\ + c_{74}u_1(t-\tau_1-\tau_6) + [c_{75}x_1(t-\tau_6) + c_{76}] \cdot \\ [1 - c_{77}x_3(t-\tau_6)]/[x_3(t-\tau_6)\{x_1(t-\tau_6) + c_{78}\}] + c_{79}, \quad (45)$$

where x_1 is the drum pressure (kgf/cm^2), y_1 is the measured drum pressure (PSI), y_2 and x_2 are the measured excess oxygen level (%) and its state (%), respectively, x_3 is the system fluid density (kg/m^3), y_3 is the drum water level (in), x_4 is the exogenous variable related to the load disturbance intensity which takes value between 0 and 1, u_1, u_2, and u_3 are, respectively, the fuel, air, and feed water flow rate inputs which are scaled to take values between 0 and 1, w_d is the load level, c_{ij} are constants, and τ_i ($i = 1, …, 6$) are delay times. Let the input and output vectors be $\boldsymbol{u}_{p0}=[u_1 \ u_2 \ u_3]^T$ and $\boldsymbol{y}_{p0} = [y_1 \ y_2 \ y_3]^T$, respectively. The inputs, outputs, and load level are scaled and biased to take values between 0% and 100%. Let the converted input vector be $\boldsymbol{u}_p =[u_f(t-\tau_1) \ u_f(t-\tau_2) \ u_w(t-\tau_3)]^T$, where u_f and u_w are scaled fuel and water flow rate. Note that the air flow rate is assumed to be regulated by the air control subsystem, which allows u_2 to be modelled as an affine function of u_f. Let the converted output vectors be $\boldsymbol{y}_p$ and the scaled load level be w_l.

The time delay is modelled as a first-order system by applying the first-order Padé approximation. Let the state vector of the above nonlinear model be $\boldsymbol{x}_p$ and the state vectors representing the time delay for the inputs and outputs

be $\boldsymbol{x}_{d1}$ and $\boldsymbol{x}_{d2}$, respectively. The total state vector is then given by $\boldsymbol{x}_{nl} = [\boldsymbol{x}_p^T \ \boldsymbol{x}_{d1}^T \ \boldsymbol{x}_{d2}^T]^T$.

Assuming that the nonlinear model represents the plant, the present authors have identified the plant parameters by applying the least-squares method to input-output data of the implemented Simulink® model (Morilla, 2011b). Equilibrium states, $\boldsymbol{x}_{nl}^*$, and inputs, $[u_f^* \ u_w^*]^T$, are calculated on the basis of the identified model and the following values specified in Morilla (2011b): $\boldsymbol{y}_p^* = [60 \ 50 \ 50]^{T}\%$ and $w_l^* = 46.36\%$.

Linearizing the nonlinear model around the equilibrium point and using the states for the time delays yields the following 10th-order linear model:

$$\dot{x}(t) = Ax(t) + Bu(t) + E_p[w_l(t) - w_l^*], \quad (46)$$

$$y(t) = Cx(t) + Du(t), \quad (47)$$

where $\boldsymbol{x}(t) = \boldsymbol{x}_{nl}(t) - \boldsymbol{x}_{nl}^*$, $\boldsymbol{u}(t) = [u_f(t) \ u_w(t)]^T - [u_f^* \ u_w^*]^T$, $\boldsymbol{y}(t) = \boldsymbol{y}_p(t) - \boldsymbol{y}_p^*$, and the coefficient matrices are defined as

$$A = \begin{bmatrix} A_p & 2B_p & 0_{4\times4} \\ 0_{3\times4} & -T_1 & 0_{3\times4} \\ T_4C & 2T_4D & -T_4 \end{bmatrix}, \quad B = \begin{bmatrix} -B_pT_3 \\ T_2 \\ -T_4DT_3 \end{bmatrix},$$

$C = [-C_p \ -2D \ 2I_3]$, and $D = D_pT_3$.

In the above matrices, $0_{p\times q}$ denotes a $p\times q$ zero-matrix and other sub-matrices are given as follows:

$$A_p = -\begin{bmatrix} 4.1693 & 0 & 0 & 324.98 \\ 0 & 228.62 & 0 & 0 \\ 20.548 & 0 & 0 & 588.41 \\ 0 & 0 & 0 & 40.000 \end{bmatrix} \times 10^{-3},$$

$$B_p = \begin{bmatrix} 25.235 & 0 & -1.3487 \\ -726.61 & 726.60 & 0 \\ 0 & 0 & 78.148 \\ 2.7027 & 0 & 0 \end{bmatrix} \times 10^{-4},$$

$$C_p = \begin{bmatrix} 5.0000 & 0 & 0 & 0 \\ 0 & 20.000 & 0 & 0 \\ 0.86013 & 0 & 1.4478 & 109.01 \end{bmatrix},$$

$$D_p = \begin{bmatrix} 0 & 0 & 0 \\ 0 & 0 & 0 \\ 0.11464 & 0 & -0.020808 \end{bmatrix}, \quad E_p = [0 \ 0 \ 0 \ 7.9958\times10^{-5}]^T,$$

$T_1 = \text{diag}(2/\tau_1, 2/\tau_2, 2/\tau_3)$, $T_4 = \text{diag}(2/\tau_4, 2/\tau_5, 2/\tau_6)$,

$$T_2 = \begin{bmatrix} 2/\tau_1 & 0 \\ 2/\tau_2 & 0 \\ 0 & 2/\tau_3 \end{bmatrix}, \quad T_3 = \begin{bmatrix} 1 & 0 \\ 1 & 0 \\ 0 & 1 \end{bmatrix},$$

where the delay times are $\tau_1=\tau_2=2$, $\tau_3=\tau_4=3$, $\tau_5=4$, and $\tau_6=2$.

3.2 Controller Design and Simulation

Since the model has dc-elements as shown in (47), the first-order dynamics, $1/(0.1s+1)$, is added in series at the inputs. The filter, however, is used only in controller design, and not used in robust stability analysis and nonlinear simulation. The resulting model becomes of the 12th order. Although y_2 is measured, the outputs to be controlled are y_1 and y_3 only. The output vector is then redefined as $\boldsymbol{y}=[y_1 \ y_3]^T$. Accordingly, the second rows of $\boldsymbol{C}$ and $\boldsymbol{D}$ are removed in the plant model

for controller design. In the following the I-P controller of (36) is designed, and then converted into the PI-type of (37), in which $y = y_I$; hence, y_P, y_{PD}, and y_D are null. In order to avoid a problem with numerical computation, the model is reduced to the ninth order by truncating the states corresponding to the Hankel singular values smaller than 10^{-15} with FBR.

An IOS is synthesized for the ninth-order model with the weighting matrices: $Q_y = I_2$ and Q_ε = diag(0.12, 0.06), which are selected by trial-and-error, as is the case with LQR design. Applying BT to the IOS and reducing the dimension of x to two yields the PI gain matrices:

$$K_P = \begin{bmatrix} -1.6495 & -1.2606 \\ 10.957 & -2.4574 \end{bmatrix}, \; K_I = \begin{bmatrix} 0.095153 & 0.036558 \\ -0.073116 & 0.047577 \end{bmatrix}$$

Let this controller be Controller A. For comparison, simulation was also conducted using the two controllers shown in Morilla (2011a). One controller, which is used for reference, has the PI gains, K_P = diag (2.5, 1.25) and K_I = K_P/50 and the other PI controller for evaluation has the gains, K_P = diag (5.0, 2.5) and K_I = K_P/25. Let the latter controller be Controller B. These controllers are the decentralized type.

Tables 2, 3 and 4, in which ω_c denotes the gain crossover frequency, summarize the stability margins of the controllers. Although part of the stability margins of the proposed PI controller are smaller than those of the decentralized controllers, the phase margin of the proposed PI controller for the open-loop system broken at u_2 or y_3 is considerably larger, which makes the time responses of y_3 less oscillatory. The generalized stability margin (Vinnicombe, 2001), which is a criterion of robust stability for MIMO systems, is also computed to be 0.06472 for Controller A, 0.05519 for Controller B, and 0.1467 for the reference controller. Hence, Controller A is probably more robust than Controller B in the MIMO environment.

Table 2 Stability Margins (Evaluated PI controller A)

Breaking the loop at	Gain Margin	Phase Margin	ω_c (rad/s)
u_1	10.68 dB	68.83 deg	0.06442
u_2	10.39 dB	52.55 deg	0.04394
y_1	21.40 dB	57.64 deg	0.04186
y_3	12.62 dB	63.44 deg	0.06615

Table 3 Stability Margins (Reference PI controller)

Breaking the loop at	Gain Margin	Phase Margin	ω_c (rad/s)
u_1 (y_1)	20.97	92.45 deg	0.02377
u_2 (y_3)	27.69	39.33 deg	0.02122

Table 4 Stability Margins (Evaluated PI controller B)

Breaking the loop at	Gain Margin	Phase Margin	ω_c (rad/s)
u_1 (y_1)	14.68	64.02 deg	0.06220
u_2 (y_3)	20.48	31.59 deg	0.04298

Nonlinear simulation results for step and ramp changes of the load level, and step change of the set point of the steam pressure are shown in Figs. 1, 2, and 3, respectively. The evaluation indexes of control performance of the controllers relative to that of the reference controller, such as the ratio of integrated absolute error (RIAE), are summarized in Tables 5, 6, and 7. Each index is defined in Morilla (2011a). The sampling period is set to 5s for Controllers A and B and 10s for the reference controller. Although the control error in the

response of y_3 to the ramp change is larger as shown in Fig. 2, which results in the increase of the combined index, J_M, as a whole the control performance of Controller A is better than that of Controller B.

Table 5 Evaluation indexes corresponding to the test of Fig. 1

Controller	RIAE$_1$	RIAE$_2$	RIAE$_3$	RIAVU$_1$	RIAVU$_2$	J$_M$
A	0.1661	1.001	0.4622	1.340	2.791	0.7604
B	0.2682	0.9993	0.4954	1.614	2.651	0.8083

Table 6 Evaluation indexes corresponding to the test of Fig. 2

Controller	RIAE$_1$	RIAE$_2$	RIAE$_3$	RIAVU$_1$	RIAVU$_2$	J$_M$
A	0.1560	1.025	0.5445	1.197	2.706	0.7718
B	0.2630	0.9996	0.3101	1.498	1.654	0.6745

Table 7 Evaluation indexes corresponding to the test of Fig. 3

C	RIAE$_1$	RIAE$_2$	RIAE$_3$	RITAE$_1$	RIAVU$_1$	RIAVU$_2$	J$_M$
A	0.4405	1.068	0.1807	0.2743	1.732	2.666	0.6805
B	0.5250	1.154	1.130	0.3696	2.626	4.449	1.099

4. CONCLUSIONS

The proposed method is basically composed of two steps: design and truncation of an IOS, i.e., design and reduction of a higher-order controller. The simple method makes design of a centralized PID controller highly efficient, allowing gain adjustment through selection of the weighting matrices of the IOS. A notable feature of the method is that part of the outputs that are not required to track reference outputs can be used for P action only, although this feature was not taken advantage of in the design example, since the excess oxygen level is a noisy measurement and does not affect other states. This feature is also true of the design method based on plant reduction by FBR (Kondo, Ochi, and Sasano, 2010). A future work is to make a comparative study about merits and demerits of each design method.

REFERENCES

Anderson, B. and Liu, Y. (1989). Controller reduction: concepts and approach. *IEEE Trans. Automatic Control*. vol. 34, pp. 802-812.

Åström, K. and Hägglund, T. (2006). *Advanced PID Control*, ISA, Research Triangle Park.

Codrons, B. (2005). *Process modelling for control*. Springer, London.

Johnson, M. and Moradi, H. (ed.) (2005). PID *Control –New Identification and Design Methods*, Ch. 11. Springer, London.

Kondo, H., Ochi, Y., and Sasano, S. (2011), PID controller design using fractional balanced reduction. *Proc. of SICE Annual Conference 2011*, Tokyo, pp. 1791-1796.

Meyer, D. (1990). Fractional balanced reduction: model reduction via fractional representation. *IEEE Trans. Automatic Control*, vol. 35, pp. 1341-1345.

Moore, B. (1981). Principal component analysis in linear systems: controllability, observability, and model reduction. *IEEE Trans. Automatic Control*, vol. 26, pp. 17-32.

Morilla, F. (2011a). Benchmark for PID control based on the boiler control problem. URL: http://www.dia.uned.es/~fmorilla/benchmarkPID2012/BenchmarkPID2012.pdf

Morilla, F. (2011b). The Matlab & Simulink files to approach the boiler control problem. URL: http://www.dia.uned.es/~fmorilla/benchmarkPID2012/BenchmarkPID2012 files.pdf

Ochi, Y. and Kondo, H. (2010). PID controller design based on optimal servo and ν-gap metric. *Proc. of the 2010 American Control Conference*, Baltimore, pp. 1091-1096.

Seraji, H. (1980). Design of multivariable PID controllers for pole placement, *International J. Control*, vol. 32, pp. 661-668.

Silva, E. and Erraz, D. (2006). An LQR based MIMO PID controller synthesis method for unconstrained Lagrangian mechanical systems. *Proc. of the 45th IEEE Conference on Decision and Control*, San Diego, pp. 6593-6598.

Smith, H. and Davison, E. (1972). Design of industrial regulators. *Proceedings of IEE*, vol. 119, pp. 1210- 1216, August.

Suh, B. and Yang, J. (2005). A tuning of PID regulators via LQR approach, *J. Chemical Eng. of Japan*, vol. 38, pp. 344-356.

Vinnicombe, G. (1993). Frequency domain uncertainty and the graph topology. *IEEE Trans. Automatic Control*, vol. 38, pp. 1371-1383.

Vinnicombe, G. (2001). *Uncertainty and Feedback*, Chapter 3. Imperial College Press, London.

Zheng, F, Wang, Q., and Lee. T. (2002). On the design of multivariable PID controllers via LMI approach, *Automatica*, vol. 38, pp. 517-526.
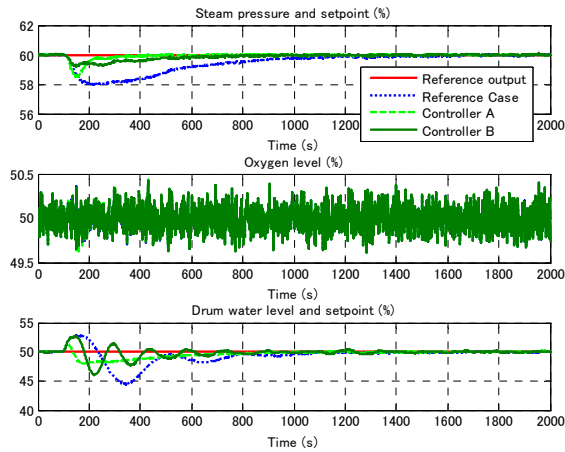
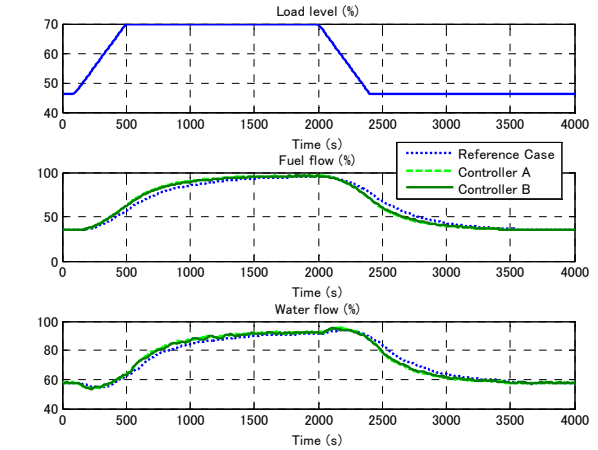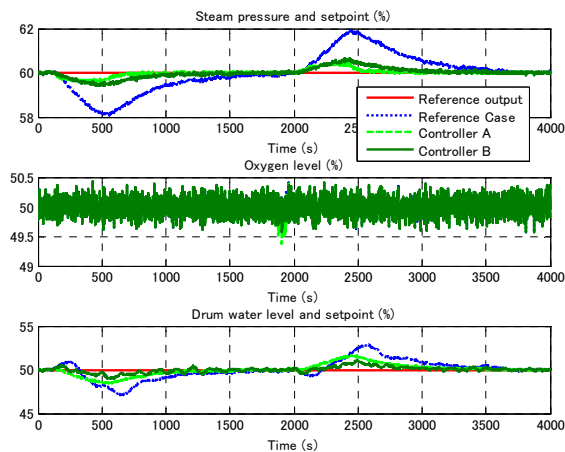Fig. 2 Time responses to the ramp change of load level
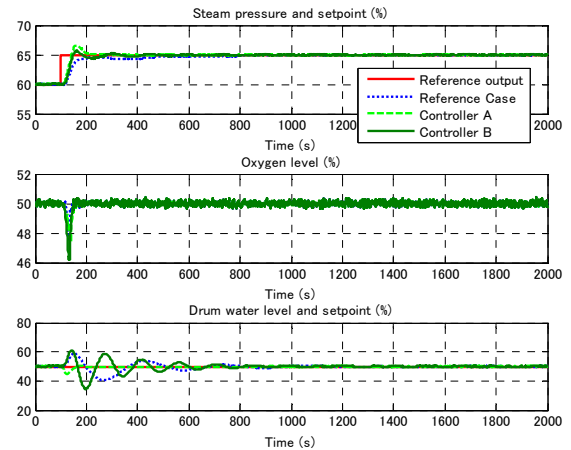
Fig. 1 Time responses to 20% step change of load level

Fig. 3 Time responses to 5% step change of steam pressure